

Satellite observations cap the atmospheric organic aerosol budget

Colette L. Heald,¹ David A. Ridley,¹ Sonia M. Kreidenweis,¹ and Easan E. Drury²

Received 13 August 2010; revised 5 October 2010; accepted 14 October 2010; published 24 December 2010.

[1] Limited understanding of the production and loss of organic aerosol (OA) to the atmosphere has resulted in poorly constrained source estimates ranging from 140 to 910 TgCyr⁻¹ [Goldstein and Galbally, 2007]. We use satellite observations to quantitatively estimate the atmospheric burden of organic aerosol and the associated production. We find that attributing the mid-visible continental aerosol optical depth (AOD) observed by the MISR satellite entirely to OA implies a global source of 430 TgCyr⁻¹ of sub-micron OA. We use a model (GEOS-Chem) to remove the contribution of inorganic aerosol, dust and soot from the observed AOD and derive a continental OA production of 150 TgCyr⁻¹ (equivalent burden of 2.5 TgC), with 80% uncertainty. This result significantly reduces the uncertainty in the global OA budget and provides an upper limit for the “missing source” of OA. **Citation:** Heald, C. L., D. A. Ridley, S. M. Kreidenweis, and E. E. Drury (2010), Satellite observations cap the atmospheric organic aerosol budget, *Geophys. Res. Lett.*, 37, L24808, doi:10.1029/2010GL045095.

1. Introduction

[2] Particles in the atmosphere affect the radiation balance of the Earth and are deleterious to human health. Measurements of organic aerosol (OA) suggest that these particles make up an important, sometimes dominant, fraction of fine particle mass in the atmosphere [Zhang *et al.*, 2007]. However poor understanding of the formation and evolution of OA in the atmosphere, as well as limited measurements of organic aerosol throughout the troposphere, translate to large uncertainties on the global OA budget. Source estimates occupy a wide range of values from 140 to 910 TgCyr⁻¹ [Goldstein and Galbally, 2007]. These estimates exceed sources included in current models (e.g., 47 TgCyr⁻¹ [Henze *et al.*, 2008]). While some field studies support a large missing source of OA in models [de Gouw *et al.*, 2005; Heald *et al.*, 2005; Johnson *et al.*, 2006; Volkamer *et al.*, 2006], others report good agreement between simulated and measured concentrations [Capes *et al.*, 2009; Chen *et al.*, 2009; Dunlea *et al.*, 2008; Heald *et al.*, 2006]. We use satellite observations to investigate whether there is evidence for a sizeable missing source of OA.

[3] The atmospheric burden of OA currently estimated using models is comparable to the burden of sulfate [Intergovernmental Panel on Climate Change, 2007], which by scattering solar radiation acts to cool the Earth and counter some of the warming from greenhouse gases. The International Governmental Panel on Climate Change estimates that

emissions of sulfur dioxide (the precursor to sulfate) will decline in coming decades with the implementation of control technologies and the use of cleaner fuels [Nakicenov *et al.*, 2000]. While an aerosol clean-up has clear air quality benefits, it may accelerate some of the GHG warming “in the pipeline” [Andreae *et al.*, 2005]. This potential effect intensifies the need to understand the budgets of aerosols in the atmosphere which share the scattering properties of sulfate.

[4] Organic aerosol can be directly emitted to the atmosphere from combustion or biological sources (known as primary OA) or it can be formed from the oxidation of semi-volatile organic gases (known as secondary OA). While state-of-the-art models include both of these source types, the pathways of SOA formation are not well understood, and may be underestimated [Hallquist *et al.*, 2009]. Goldstein and Galbally [2007] propose a large possible range of global SOA sources (140–910 TgCyr⁻¹) based on several mass balance calculations. Not all of their calculations are specific to SOA, and given the challenges in distinguishing SOA and POA from observations, we take this number to be the range of possible OA sources. One of the approaches used in their study derived the OA source by scaling the sulfate source, resulting in an OA source estimate of 140–540 TgCyr⁻¹. This estimate was refined by Hallquist *et al.* [2009] who used a more modest OA to sulfate ratio to calculate a range of 60–240 TgCyr⁻¹. The observed OA to sulfate ratio is highly variable; ratios for the surface observations reported by Zhang *et al.* [2007] range from 0.3 to 7.0. Given that sulfate and OA only share a subset of their many sources and formation pathways, sulfate production is not a good proxy for the OA source, and thus the uncertainty on this approach is very large.

[5] Our objective is to quantitatively constrain the range of the global OA source. Measurements of OA concentrations are largely limited to easily accessible surface sites in the Northern Hemisphere [Zhang *et al.*, 2007]. These in situ observations do not adequately characterize the global continental composition of the troposphere, particularly the free troposphere where OA sources aloft may enhance the total burden [Goldstein *et al.*, 2009; Heald *et al.*, 2005; Morgan *et al.*, 2009]. Satellites, however can provide both a total integrated measurement of the aerosol column (aerosol optical depth) as well as a near-continuous, global view of aerosol loading. The penalty is that AOD is an integrated measure of extinction from all the particles in the atmosphere, and thus uncertainties on the derived contribution from any specific particle type will be high. We focus here on continental sources of OA and the constraints offered by satellite observations over land.

2. Methods

[6] We use measurements from the Multi-angle Imaging SpectroRadiometer (MISR) [Diner *et al.*, 1998] satellite instrument which uses multi-angle measurements in the

¹Department of Atmospheric Science, Colorado State University, Fort Collins, Colorado, USA.

²National Renewable Energies Laboratory, Golden, Colorado, USA.

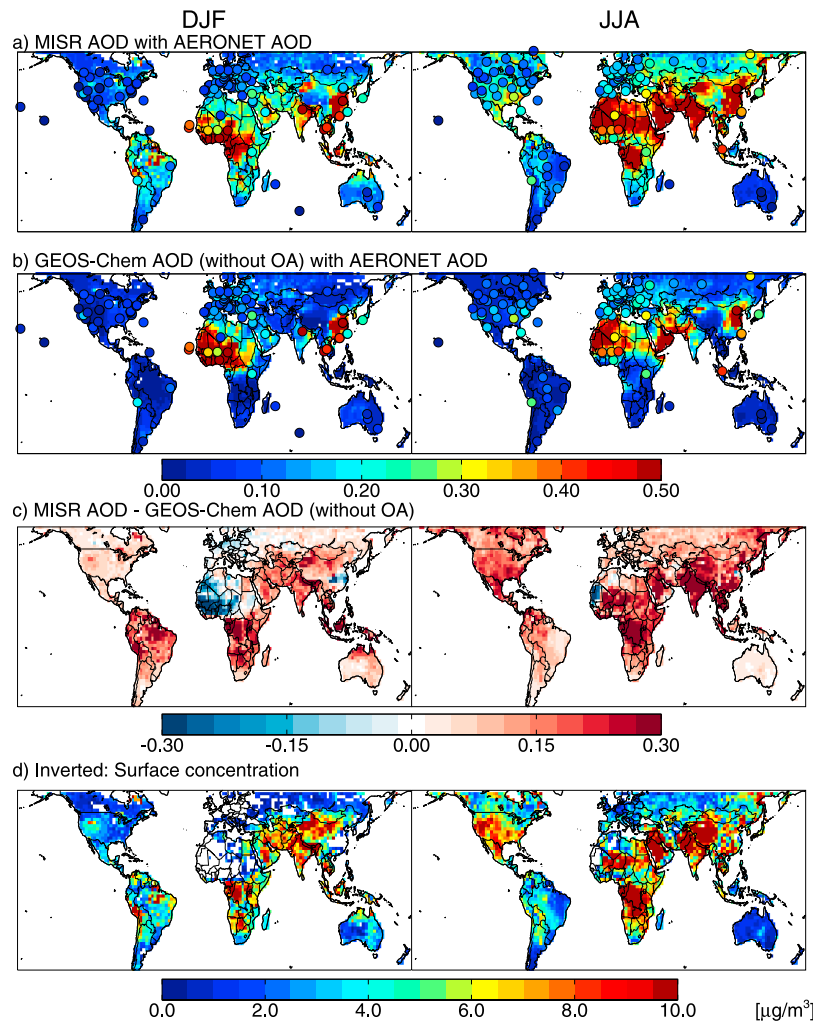


Figure 1. Total aerosol optical depth for (left) winter and (right) summer 2008 as (a) measured by MISR at 555 nm and (b) simulated by the GEOS-Chem model at 555 nm (without OA) as sampled for the MISR overpass (AERONET ground-based sunphotometer network observations at 550 nm overlaid in Figure 1a). (c) The difference and (d) the inverted surface concentrations when assuming a constant mixing ratio profile.

visible to near-IR to retrieve AOD. Observations shown here correspond to the 2008 Level 3, version 15, daily AOD product at 555 nm and are re-gridded to seasonal means at $2^\circ \times 2.5^\circ$ spatial resolution. Figure 1 shows a comparison of winter and summer mean continental AOD reported by MISR with the AERONET network of sunphotometer sites [Holben *et al.*, 1998] and the GEOS-Chem global chemical transport model, excluding OA. AERONET observations shown here are seasonal means, sampled to coincide with the MISR local overpass time, of the Level 2 (quality assured) 2008 data, interpolated to 550 nm. We use v8-02-04 of the GEOS-Chem model (www.geos-chem.org) driven by GEOS-5 meteorology for the year 2008. The GEOS-Chem coupled aerosol-oxidant simulation includes H_2SO_4 - HNO_3 - NH_3 aerosol thermodynamics coupled to an ozone- NO_x -hydrocarbon-aerosol chemical mechanism [Park *et al.*, 2004]. The model scheme also includes black carbon [Park *et al.*, 2003], sea salt aerosol (fine and coarse) [Alexander *et al.*, 2005], and soil dust [Fairlie *et al.*, 2007]. All aerosols are treated as externally mixed with log-normal size distributions and mass extinction efficiencies are calculated as a function of relative humidity as described by Martin *et al.* [2003]. Aerosol optical

properties (including refractive indices and aerosol growth factors) employed here are based on the Global Aerosol Data Set (GADS) [Kopke *et al.*, 1997] with modifications to the size distribution from Drury *et al.* [2010] based on field observations (Figure S1 of the auxiliary material shows the mass extinction efficiencies used for continental aerosol at 550 nm).¹ The model simulation is sampled for the MISR overpass time ($\sim 10:30\text{am}$) and location in Figure 1. This comparison confirms a widespread underestimate of continental AOD in the model which spans both urban and remote environments. Previous evaluation of speciated aerosol concentrations suggests that the GEOS-Chem model provides a robust description of aerosol concentrations (other than OA) [Drury *et al.*, 2010; Fairlie *et al.*, 2007; Park *et al.*, 2004, 2005]. Regions which are overestimated in the model (Figure 1) are generally associated with dust (or dust transport), in common with many models [Kinne *et al.*, 2006]. We use MISR AOD observations to constrain the global OA budget; comparisons with AERONET and MODIS are shown in Supplementary

¹Auxiliary materials are available in the HTML. doi:10.1029/2010GL045095.

Table 1. Uncertainty, Estimated 95% Confidence Intervals, in Inferred Organic Aerosol Source

Factors	Uncertainty
Aerosol optical properties	50%
Size parameters	20%
Refractive indices	10%
Aerosol water uptake (growth factor)	6% ^a
Relative humidity (assuming 5% uncertainty in GEOS-5 fields)	
Conversion from burden to source	50%
Aerosol lifetime (including effects of vertical profile and export fraction)	
Global budget of “other” aerosols simulated in GEOS-Chem	25%
MISR AOD measurements	10%
Total Uncertainty (added in quadrature)	80%

^aUnless RH > 90% in which case uncertainty is significantly large (~50%)

Materials (Figures S2–S4). A detailed error analysis follows these estimates.

[7] AOD is related to the mass concentration profile ($M(z)$) via the mass extinction efficiency (α):

$$\text{AOD} = \int_0^{z_{\text{top}}} \alpha(\text{RH}(z))M(z)dz \quad (1)$$

The dependence of the mass extinction efficiency on relative humidity reflects aerosol uptake of water. To invert observed AOD for atmospheric burden, we start with a uniform $1 \mu\text{gsm}^{-3}$ tropospheric profile of OA (at Standard Temperature and Pressure, uniform in mixing ratio) and using relative humidity from the GEOS-5 re-analysis product, apply the appropriate α to estimate seasonal mean maps of the associated AOD for every grid box. These AOD are scaled to match the MISR observations, and from this an OA burden is derived. This burden is translated to a source estimate by assuming a 6 day lifetime for atmospheric OA, consistent with the mean OA lifetime simulated by Henze *et al.* [2008]. We use seasonal maps to ensure the most complete global coverage. The optical properties used here (see Figure S1) are for sub-micron OA. Coarse OA, such as large primary biological aerosol particles (PBAP), is significantly less optically effective in the mid-visible, and is therefore not included in the budget estimated here. This may overestimate the contribution of sub-micron OA in localized regions of high coarse PBAP loading.

3. Results

[8] If we assume that OA makes up the entire AOD and invert for the burden implied by the continental MISR observations, we estimate a source of 215 TgCyr^{-1} . This source must be doubled to account for the continental OA exported in outflow (based on a GEOS-Chem model estimate that 40–60% of OA is exported over the ocean). The continental OA burden required to account for the AOD observed by MISR is therefore estimated at a maximum of 7.0 TgC (associated source of 430 TgCyr^{-1}). This reduces the likely range of OA sources by more than half.

[9] This estimate neglects the known presence of other aerosols such as dust, sulfate and soot in the atmosphere. To

refine this assessment, we invert the seasonal difference between MISR observed AOD and the simulated total AOD in the GEOS-Chem model (excluding OA). This assumes that all the negative bias in the model simulation can be attributed to OA sources. Scaling to account for outflow, the OA source required to explain the observed-modeled AOD discrepancy is 210 TgCyr^{-1} . The inverted concentrations are shown in Figure 1d. The geographical distribution of this inverted OA is illustrative, and represents a maximum potential OA for all locations, given that poor model representation of other particle types would be mistakenly ascribed to OA here. In particular, model underestimates of summertime AOD over Northern Africa and the Middle East can most likely be attributed to underestimated dust sources, and not organics. Removing these regions ($0\text{--}35^\circ\text{N}$, $20^\circ\text{W}\text{--}50^\circ\text{E}$) from the inversion, the source is further reduced to 170 TgCyr^{-1} .

[10] A uniform vertical mixing ratio of OA was specified for simplicity when inverting the AOD. Such a profile seems unlikely given the efficient removal of OA in precipitating air masses, however additional production aloft may provide a compensatory source. There are few constraints on the vertical profile of OA in the atmosphere [Capes *et al.*, 2009; DeCarlo *et al.*, 2008; Dunlea *et al.*, 2008; Heald *et al.*, 2005, 2006; Morgan *et al.*, 2009]. For the purpose of calculating the OA budget we therefore invoke an intermediate vertical distribution: an exponentially decreasing profile characterized by the scale height of the atmosphere. When the same mass in the uniform profile is re-distributed to such a shape the global mean AOD increases by 15% due to additional water uptake near the surface. As a result, 15% less mass would be required to match the MISR observations. Our optimized continental OA source therefore totals 150 TgCyr^{-1} (equivalent atmospheric burden of 2.5 TgC).

[11] Surface concentrations of OA are not well constrained by this assessment of the global burden, given the uncertainty in the vertical distribution of OA at each location. For example, the vertical distribution described above implies surface concentrations double the values shown in Figure 1d. Indeed, we have argued that surface concentrations do not provide a strong constraint on the global OA budget, and thus the converse must also be true. As a result, comparison with a suite of surface OA measurements only confirms that the OA source is likely to be higher than current model sources (47 TgCyr^{-1}) and less than the OA estimated when the entire AOD is inverted (430 TgCyr^{-1}) (Figure S5 of the auxiliary material).

4. Uncertainties

[12] Using AOD to constrain the OA source implies substantial uncertainties on the derived budget. Table 1 summarizes the factors contributing to these uncertainties (estimated 95% confidence intervals). The most important factors are the OA optical properties used to convert from AOD to mass and the OA lifetime assessed to convert the burden to a global source.

[13] Our production estimates are based on an intermediate OA lifetime of 6 days, with a likely range of 4–8 days translating to a 50% uncertainty. The uncertainty associated with the assumed vertical profile and the fraction of OA exported are estimated at 15% and 20%, however these factors are all coupled with the OA lifetime and are to some

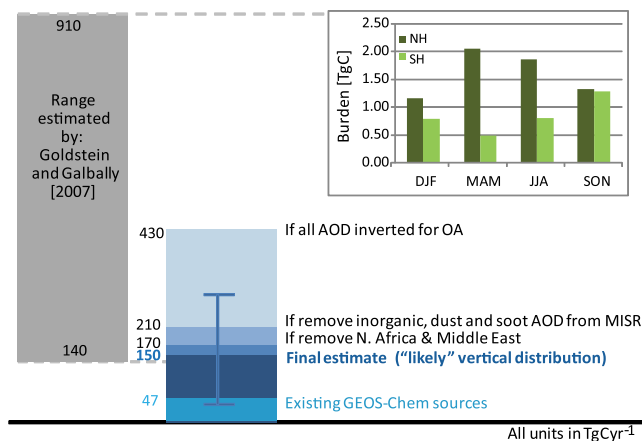


Figure 2. Continental OA source estimates derived here compared with the estimates of *Goldstein and Galbally* [2007]. Seasonality of the estimated burden is shown in the inset.

degree, mitigating. For example, a greater fraction of aerosol aloft would require an increase in the source for the same observed AOD, but would be associated with a longer aerosol lifetime, which would imply a decreased source, as well as a larger fraction of exported aerosol, which would imply an increased source. Thus, we assume that the 50% uncertainty on lifetime incorporates the uncertainty in the vertical profile and export fractions.

[14] Figure S6 shows the sensitivity of the mass extinction efficiency of OA at 550 nm to assumed size and optical properties calculated using Mie code. The optical properties are most sensitive to the size of the aerosol, with an associated uncertainty of 50%. To test the sensitivity of our AOD calculations to assumed refractive index we use a series of literature values for dry refractive index for OA, and calculate refractive indices at higher relative humidities following volume mixing rules [Stelson, 1990]. These dry refractive indices include values suggested by *Jacobson* [2005] and used in the GOCART model [Chin et al., 2002]. We also test the difference in mass extinction efficiency produced when the dry refractive indices determined for several types of HULIS [Dinar et al., 2008] or Suwannee River Fulvic Acid [Lang-Yona et al., 2009] are employed. The calculated mass extinction efficiencies all fall within 20% of our standard values. Note that uncertainty associated with the organic refractive index is highest at low relative humidity, where organic material makes up more of the aerosol mass. The OA growth factor ($GF = D_{wet}/D_{dry}$) at 90% used here (1.6) is less than typical values for sulfate (1.7–1.8), higher than environments characterized by biomass burning (1.2–1.3), and at the higher end of GF observed in rural environments [Swietlicki et al., 2008] and is thus likely representative of well-aged OA. Given uncertainties regarding how mixing state and organic composition may affect the water uptake of organic aerosol, we estimate a 20% uncertainty in GF. We use volume mixing rules [Stelson, 1990] to calculate the resulting changes in refractive indices, and use these together with changes in size to calculate that the uncertainty in mass extinction efficiency due to the uptake in water is less than 10%. Uncertainties in relative humidity (estimated at 5%) translate to modest uncertainties in extinction efficiency for

most continental regions, but can rival the uncertainty associated with optics and lifetime in very humid regions.

[15] The MISR AOD retrieval has a 20% uncertainty on individual observations [Kahn et al., 2005]. We expect uncertainties to be considerably lower for the seasonal averages used here, and estimate this at 10%. We note that satellite observations of AOD are clear-sky only. This may underestimate the total OA burden if a significant fraction is found in-cloud, for example, due to aqueous phase production, or in the case where persistent clouds coincide with peak OA over a particular region and season. Finally, we assess a 25% uncertainty in the global seasonal AOD calculated for inorganics, dust and soot in the GEOS-Chem model. This is consistent with the total AOD diversity for the sum of these species estimated for the suite of models in the AEROCOM intercomparison [Kinne et al., 2006]. Note that uncertainties on the simulated AOD may be higher for specific locations or days.

[16] As a result of all these factors, we assess a likely maximum of 150 $TgCyr^{-1}$ continental OA source with an 80% uncertainty. The uncertainty on the derived burden is slightly lower (60%) as aerosol lifetime plays a limited role on this estimation.

5. Conclusions

[17] Despite large uncertainties, we show that the OA budget can be usefully constrained based on satellite observations. Figure 2 illustrates how the estimate derived here occupies the lowest values within the range of OA sources proposed by *Goldstein and Galbally* [2007]. While the “missing source” of OA assessed here is modest in comparison, it is a factor of two to three higher than sources included in current models. This empirical estimate cannot be used to decipher the mechanisms of OA production, however the seasonality of the inverted source (which peaks in local Spring/Summer, inset of Figure 2) hints at a relationship to biogenic activity (including summer wildfires) or enhanced photochemical activity. Attribution of this seasonality is key not only to understanding formation mechanisms, but also the broader question of what fraction of OA is natural in origin. Characterization of the aerosol composition of the global atmosphere, including the contribution from OA, is critical to our ability to predict the future radiative equilibrium of the Earth.

[18] **Acknowledgments.** This work was supported in part by NASA grant NNX08AN75G. We thank the AERONET investigators for establishing and maintaining the sites used in this investigation as well as the MISR retrieval team for providing satellite data.

References

- Alexander, B., R. J. Park, D. J. Jacob, Q. B. Li, R. M. Yantosca, J. Savarino, C. C. W. Lee, and M. H. Thiemens (2005), Sulfate formation in sea-salt aerosols: Constraints from oxygen isotopes, *J. Geophys. Res.*, *110*, D10307, doi:10.1029/2004JD005659.
- Andreae, M. O., et al. (2005), Strong present-day aerosol cooling implies a hot future, *Nature*, *435*(7046), 1187–1190, doi:10.1038/nature03671.
- Capes, G., et al. (2009), Secondary organic aerosol from biogenic VOCs over West Africa during AMMA, *Atmos. Chem. Phys.*, *9*(12), 3841–3850, doi:10.5194/acp-9-3841-2009.
- Chen, Q., et al. (2009), Mass spectral characterization of submicron biogenic organic particles in the Amazon Basin, *Geophys. Res. Lett.*, *36*, L20806, doi:10.1029/2009GL039880.
- Chin, M., et al. (2002), Tropospheric aerosol optical thickness from the GOCART model and comparisons with satellite and Sun photometer

- measurements, *J. Atmos. Sci.*, 59(3), 461–483, doi:10.1175/1520-0469(2002)059<0461:TAOTFT>2.0.CO;2.
- DeCarlo, P. F., et al. (2008), Fast airborne aerosol size and chemistry measurements above Mexico City and central Mexico during the MILAGRO campaign, *Atmos. Chem. Phys.*, 8(14), 4027–4048, doi:10.5194/acp-8-4027-2008.
- de Gouw, J. A., et al. (2005), Budget of organic carbon in a polluted atmosphere: Results from the New England Air Quality Study in 2002, *J. Geophys. Res.*, 110, D16305, doi:10.1029/2004JD005623.
- Dinar, E., et al. (2008), The complex refractive index of atmospheric and model humic-like substances (HULIS) retrieved by a cavity ring down aerosol spectrometer (CRD-AS), *Faraday Discuss.*, 137, 279–295, doi:10.1039/b703111d.
- Diner, D. J., et al. (1998), Multi-angle Imaging SpectroRadiometer (MISR)—Instrument description and experiment overview, *IEEE Trans. Geosci. Remote Sens.*, 36(4), 1072–1087, doi:10.1109/36.700992.
- Drury, E., D. J. Jacob, R. J. D. Spurr, J. Wang, Y. Shinozuka, B. E. Anderson, A. D. Clarke, J. Dibb, C. McNaughton, and R. Weber (2010), Synthesis of satellite (MODIS), aircraft (ICARTT), and surface (IMPROVE, EPA-AQS, AERONET) aerosol observations over eastern North America to improve MODIS aerosol retrievals and constrain surface aerosol concentrations and sources, *J. Geophys. Res.*, 115, D14204, doi:10.1029/2009JD012629.
- Dunlea, E. J., et al. (2008), Evolution of Asian aerosols during transpacific transport in INTEX-B, *Atmos. Chem. Phys. Discuss.*, 8, 15,375–15,461, doi:10.5194/acpd-8-15375-2008.
- Fairlie, T. D., et al. (2007), The impact of transpacific transport of mineral dust in the United States, *Atmos. Environ.*, 41(6), 1251–1266, doi:10.1016/j.atmosenv.2006.09.048.
- Goldstein, A. H., and I. E. Galbally (2007), Known and unexplored organic constituents in the Earth's atmosphere, *Environ. Sci. Technol.*, 41(5), 1514–1521, doi:10.1021/es072476p.
- Goldstein, A. H., et al. (2009), Biogenic carbon and anthropogenic pollutants combine to form a cooling haze over the southeastern United States, *Proc. Natl. Acad. Sci. U. S. A.*, 106(22), 8835–8840, doi:10.1073/pnas.0904128106.
- Hallquist, M., et al. (2009), The formation, properties and impact of secondary organic aerosol: current and emerging issues, *Atmos. Chem. Phys.*, 9(14), 5155–5236, doi:10.5194/acp-9-5155-2009.
- Heald, C. L., D. J. Jacob, R. J. Park, L. M. Russell, B. J. Huebert, J. H. Seinfeld, H. Liao, and R. J. Weber (2005), A large organic aerosol source in the free troposphere missing from current models, *Geophys. Res. Lett.*, 32, L18809, doi:10.1029/2005GL023831.
- Heald, C. L., et al. (2006), Concentrations and sources of organic carbon aerosols in the free troposphere over North America, *J. Geophys. Res.*, 111, D23S47, doi:10.1029/2006JD007705.
- Henze, D. K., et al. (2008), Global modeling of secondary organic aerosol formation from aromatic hydrocarbons: High- vs. low-yield pathways, *Atmos. Chem. Phys.*, 8, 2405–2420, doi:10.5194/acp-8-2405-2008.
- Holben, B. N., et al. (1998), AERONET - A federated instrument network and data archive for aerosol characterization, *Remote Sens. Environ.*, 66(1), 1–16, doi:10.1016/S0034-4257(98)00031-5.
- Intergovernmental Panel on Climate Change (2007), *Climate Change 2007: The Physical Science Basis. Contribution of Working Group I to the Fourth Assessment Report of the Intergovernmental Panel on Climate Change*, edited by S. Solomon et al., 996 pp., Cambridge Univ. Press, Cambridge, U. K.
- Jacobson, M. C. (2005), *Fundamental of Atmospheric Modeling*, 2nd ed., 813 pp., Cambridge Univ. Press, U. K.
- Johnson, D., et al. (2006), Simulating regional scale secondary organic aerosol formation during the TORCH 2003 campaign in the southern UK, *Atmos. Chem. Phys.*, 6, 403–418, doi:10.5194/acp-6-403-2006.
- Kahn, R. A., B. J. Gaitley, J. V. Martonchik, D. J. Diner, K. A. Crean, and B. Holben (2005), Multiangle Imaging Spectroradiometer (MISR) global aerosol optical depth validation based on 2 years of coincident Aerosol Robotic Network (AERONET) observations, *J. Geophys. Res.*, 110, D10S04, doi:10.1029/2004JD004706.
- Kinne, S., et al. (2006), An AeroCom initial assessment—Optical properties in aerosol component modules of global models, *Atmos. Chem. Phys.*, 6, 1815–1834, doi:10.5194/acp-6-1815-2006.
- Kopke, P., et al. (1997), Global aerosol data set, Max Planck Inst. für Meteorol, Hamburg, Germany.
- Lang-Yona, M., et al. (2009), Complex refractive indices of aerosols retrieved by continuous wave-cavity ring down aerosol spectrometer, *Anal. Chem.*, 81(5), 1762–1769, doi:10.1021/ac8017789.
- Martin, R. V., D. J. Jacob, R. M. Yantosca, M. Chin, and P. Ginoux (2003), Global and regional decreases in tropospheric oxidants from photochemical effects of aerosols, *J. Geophys. Res.*, 108(D3), 4097, doi:10.1029/2002JD002622.
- Morgan, W. T., et al. (2009), Vertical distribution of sub-micron aerosol chemical composition from north-western Europe and the north-east Atlantic, *Atmos. Chem. Phys.*, 9(15), 5389–5401, doi:10.5194/acp-9-5389-2009.
- Nakicenov, N., et al. (2000), *Emissions Scenarios: A Special Report of Working Group III of the Intergovernmental Panel on Climate Change*, Cambridge Univ. Press, Cambridge, U. K.
- Park, R. J., D. J. Jacob, M. Chin, and R. V. Martin (2003), Sources of carbonaceous aerosols over the United States and implications for natural visibility, *J. Geophys. Res.*, 108(D12), 4355, doi:10.1029/2002JD003190.
- Park, R. J., D. J. Jacob, B. D. Field, R. M. Yantosca, and M. Chin (2004), Natural and transboundary pollution influences on sulfate-nitrate-ammonium aerosols in the United States: Implications for policy, *J. Geophys. Res.*, 109, D15204, doi:10.1029/2003JD004473.
- Park, R. J., et al. (2005), Export efficiency of black carbon aerosol in continental outflow: Global implications, *J. Geophys. Res.*, 110, D11205, doi:10.1029/2004JD005432.
- Stelson, A. W. (1990), Urban aerosol refractive-index prediction by partial molar refraction approach, *Environ. Sci. Technol.*, 24(11), 1676–1679, doi:10.1021/es00081a008.
- Swietlicki, E., et al. (2008), Hygroscopic properties of submicrometer atmospheric aerosol particles measured with H-TDMA instruments in various environments—A review, *Tellus, Ser. B*, 60(3), 432–469.
- Volkamer, R., J. L. Jimenez, F. San Martini, K. Dzepina, Q. Zhang, D. Salcedo, L. T. Molina, D. R. Worsnop, and M. J. Molina (2006), Secondary organic aerosol formation from anthropogenic air pollution: Rapid and higher than expected, *Geophys. Res. Lett.*, 33, L17811, doi:10.1029/2006GL026899.
- Zhang, Q., et al. (2007), Ubiquity and dominance of oxygenated species in organic aerosols in anthropogenically-influenced Northern Hemisphere midlatitudes, *Geophys. Res. Lett.*, 34, L13801, doi:10.1029/2007GL029979.

E. E. Drury, National Renewable Energies Laboratory, 1617 Cole Blvd., Golden, CO 80403, USA.

C. L. Heald, S. M. Kreidenweis, and D. A. Ridley, Department of Atmospheric Science, Colorado State University, 1371 Campus Delivery, Fort Collins, CO 80525, USA. (heald@atmos.colostate.edu)